Journal of Physics: Conference Series **1435** (2020) 012030 doi:10.1088/1742-6596/1435/1/012030

Vorticity structure and polarization of Λ hyperons in heavy-ion collisions

Aleksei Zinchenko, Alexander Sorin, Oleg Teryaev, Mircea Baznat
JINR, 141980 Dubna, Russia
E-mail: zinchenko@jinr.ru

Abstract. Simulations of peripheral Au+Au collisions at NICA energies are performed in the PHSD transport model. The properties of vorticity field are studied at different impact parameters. Quadrupole structures of the vorticity field in all planes are obtained. A thin layer of large vorticity is found at the boundary of the fireball, the so-called vortex sheet. The effect of helicity separation is detected. Calculation of hyperon polarization in thermodynamic and anomalous models is performed.

1. Introduction

The experimental data of STAR collaboration [1] indicate the presence of hyperon polarization in heavy-ion collisions. There are several approaches that allow to explain and calculate this polarization. The most often used from them is performed [2] in the framework of approach exploring local equilibrium thermodynamics [3] and hydrodynamical calculations of vorticity [4].

There is another (although related [5]) approach to polarization first proposed in [6] and independently in [7]. It is based on vortical effect (see e.g. [8]) that being the macroscopic manifestation of axial anomaly [9] leads to induced axial current of strange quarks which may be converted to polarization of Λ-hyperons [6, 7]. The effect is proportional to vorticity and helicity of the strong interacting medium. Thus, vorticity of the medium contributes and determines polarization regardless of the approach, which gives the reason to explore its possible structures. It is the main goal of the work.

2. PHSD

All calculations are performed in the PHSD transport model [10]. The Parton-Hadron-String Dynamics (PHSD) is a microscopic off-shell transport approach that consistently describes the full evolution of a relativistic heavy-ion collision from the initial hard scatterings and string formation through the dynamical deconfinement phase transition to the quark-gluon plasma as well as hadronization and to the subsequent interactions in the hadronic phase. It was recently used for calculations of polarization [11].

We define velocity field as:

$$v_1^a(x) = \frac{\sum_i p_i^a F(x, x_i)}{\sum_i p_i^0 F(x, x_i)}\,, \tag{1}$$

where F is smearing function, $a = 1, 2, 3$ is the spatial indices, p_i^a and p_i^0 are the momentum and energy of the i-th particle, and the summation is over all the particles.

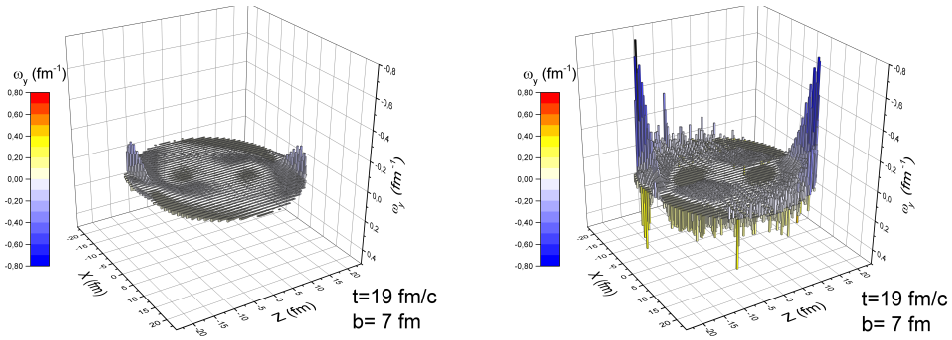

a) b)

Figure 1. Y-component of vorticity in reaction plane XZ ($y = 0$) in the case of the classical definition -a) and relativistic -b) at energy $\sqrt{s} = 7.7$ GeV.

3. Vorticity structure

There are few definitions of vorticity. We will use the non-relativistic and relativistic kinetic vorticity:

$$\varpi_{\mu\nu} = \frac{1}{2}(\partial_\nu v_\mu - \partial_\mu v_\nu)\,, \quad \omega_{\mu\nu} = \frac{1}{2}(\partial_\nu u_\mu - \partial_\mu u_\nu)\,, \tag{2}$$

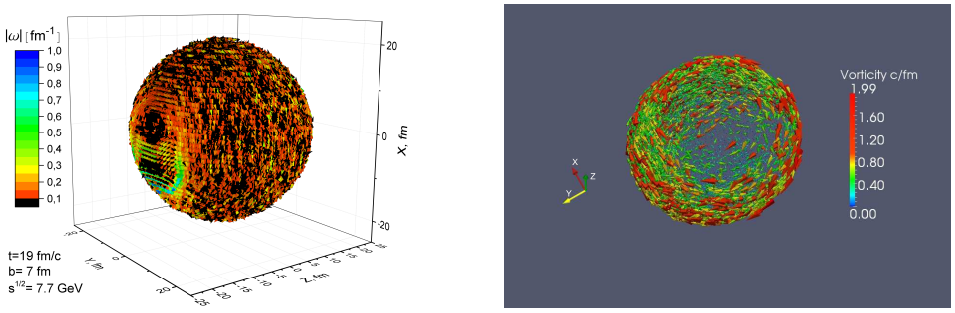

a) b)

Figure 2. Vortex sheet in the PHSD model a) and QGSM b).

where u_ν is a relativistic four-vector of the velocity field.

In the case of relativistic vorticity, γ-factor has a significant influence on the fireball boundaries, strengthening vorticity value (Fig. 1). It takes the largest value on the boundaries of fireball and spectators, and it has the same sign on both boundaries, which together gives a non-zero ω_y vorticity in the XZ plane (Fig. 1). This is quite natural, since the gold cores are not ideal liquids, and in an off-center collision a rotational moment, distinct from zero, will arise along the axis perpendicular to the reaction plane, which we observe.

The presence of many peaks in Fig. 1 and their distribution indicate the vortex sheet begins ton the boundary of the fireball at energy $\sqrt{s} = 7.7$ GeV. It is observed both in the QGSM [12] and in the PHSD model(see Fig. 2), where even at large times it has a significant vorticity on the border of participants and spectators (Fig. 1 b), Fig. 2 a).

The longitudinal component of vorticity ω_z has a mirror quadrupole structure in the XY plane (see Fig. 3, the averaging was done over the cylinder along the axis Z from 1.25 to 1.25 fm). The vector component $\vec{\omega}_\perp = (\omega_x, \omega_y)$ in the same plane behaves much more interesting. It has a symmetrical structure about the y axis in $z = 0$, but when we are moving away from the center of the fireball, an external rotation and an internal rotation in the opposite direction

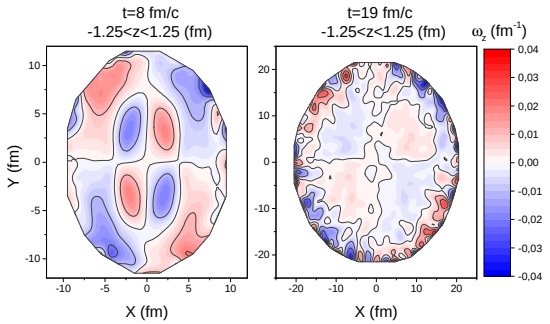

Figure 3. Quadrupole structure of relativistic vorticity ω_z in Au+Au ($\sqrt{s} = 7.7$ GeV), at different time. Averaging was performed in the 2.5 fm range in the layer $z = 0$.

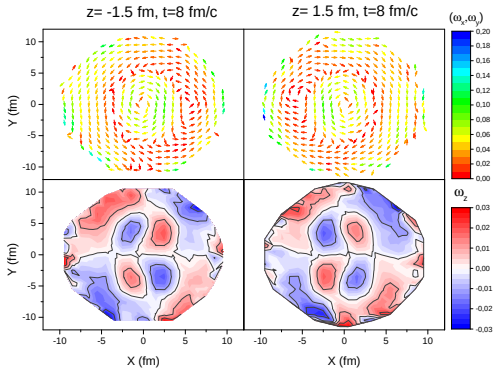

Figure 4. Quadrupole structure of relativistic vorticity ω_z in Au+Au ($\sqrt{s} = 7.7$ GeV) in the bottom line and corresponding structure of the transverse vorticity $\vec{\omega}_\perp = (\omega_x, \omega_y)$ in the same time and layer of z in the top.

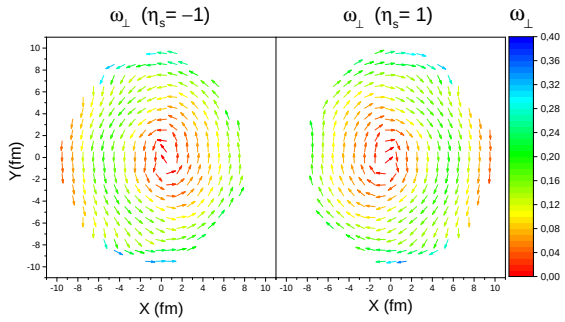

Figure 5. The distribution of the transverse vorticity $\vec{\omega}_\perp$ in the transverse plane at longitudinal position $\eta_s = -1$ (left) and $\eta_s = 1$ (right) at time $t = 9.5$ fm/c, b= 5 fm.

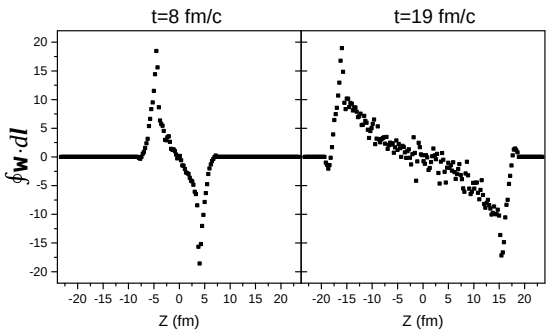

Figure 6. Vorticity field circulation in the XY plane as a function of z in different time ($b = 7$ fm, $\sqrt{s} = 7.7$ GeV).

are observed (Fig. 4). This reverse rotation exists as long as there is an internal quadrupole structure (along Z-axis). Then there remains the one-sided rotation of the vorticity vector in vertical plane, but the opposite in different signs Z. This can be seen in Fig. 5, where transverse vorticity field $\vec{\omega}_\perp$ is constructed for pseudo rapidity $\eta_s = \pm 1$ ($\eta_s = 1/2\, ln\, [(t+z)\,/\,(t-z)]$, $t = 9.5$ fm/c) and is consistent with the work [13], where similar structures for thermal vorticity are obtained.

We conclude that the vorticity field has a spherical elongated shape, at poles (along Z) of which it is maximum, and one half of this sphere rotates in one direction and the other in reverse one, having the opposite rotation in the center. Total rotation tends to zero when approaching $z = 0$. We can see this by taking the circulation of vorticity vector at various points z in XY-plane (Fig. 6). The vorticity modulus at z = 0 grows towards the boundary of the fireball and increases with time. This means that near $z = 0$ there is no distinguished direction of rotation of vorticity field, and moving away from zero, two opposite rotations are formed.

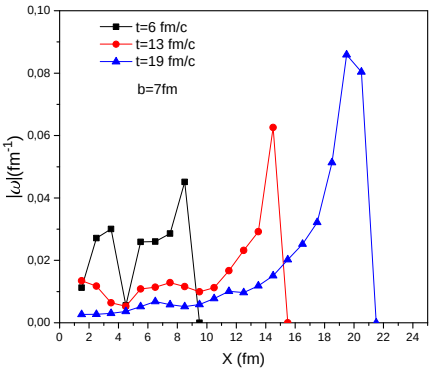

Figure 7. Dependence of the vorticity modulus on the fireball radius at different times ($b = 7$ fm, $z = 0$, $\sqrt{s} = 7.7$ GeV).

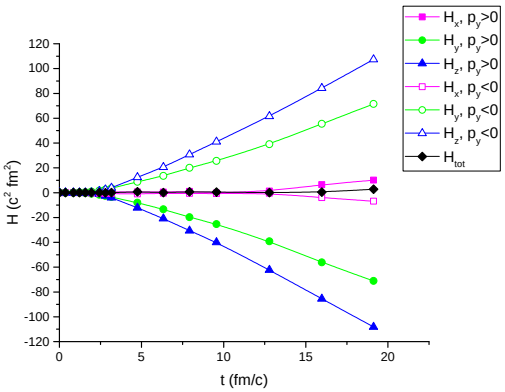

Figure 8. Separation of the helicity H component relative to y-component of momentum at different times (impact parameter $b = 7$ fm, $\sqrt{s} = 7.7$ GeV).

4. Helicity separation and Polarization

Helicity contributes directly to the polarization of hyperons in so-called axial vortical effect approach. Helicity separation effect discovered in QGSM [14], HSD [15] and PHSD model (Fig. 5) and receives the significant contribution $\sim \vec{v}_z\vec{\omega}_z$ from the longitudinal component of velocity and vorticity. Polarization is expressed in this approach (for $p_y > 0$ or $p_y < 0$) [16]:

$$< \Pi_0^\Lambda > = < \frac{m_\Lambda}{N_\Lambda\, p_y} > \frac{N_c}{2\pi^2} \int d^3x\, \mu_s^2(x) \gamma^2 \epsilon^{ijk} v_i \partial_j v_k, \qquad (3)$$

where the hydrodynamic helicity is contained within the integral $H \equiv \int d^3x (\vec{v}\cdot\vec{\omega})$. Polarization is $\Pi_0^\lambda = 0.7\%$ for thermodynamics one and $\Pi_0^\lambda = 8\%$ for anomaly approach, which is very sensitive to chemical potential ($\sqrt{s} = 7.7$ GeV). This difference can be also affected by the contribution of gravitational anomaly[17], suppressed due to the collective effects revealed in lattice simulations and the sensitivity to thermodynamic quantities.

We are grateful to E. Bratkovskaya,Yu. Ivanov, E. Kolomeitsev, V. Toneev and V. Voronyuk for useful discussions. O.T. was supported by RFBR grants 18-02-01107, 17-02-01108.

References

[1] L. Adamczyk *et al.* [STAR Collaboration] 2017 *Nature* **548** 62
[2] F. Becattini, L. Csernai and D. J. Wang 2013 *Phys. Rev. C* **88** 034905
[3] F. Becattini, L. Bucciantini, E. Grossi and L. Tinti 2015 *Eur. Phys. J. C* **75** 191
[4] L. P. Csernai, V. K. Magas and D. J. Wang 2013 *Phys. Rev. C* **87** 034906
[5] G. Prokhorov, O. Teryaev and V. Zakharov 2018 *Phys. Rev. D* **98** 071901
[6] O. Rogachevsky, A. Sorin and O. Teryaev 2010 *Phys. Rev. C* **82** 054910
[7] J. -H. Gao, Z. -T. Liang, S. Pu, Q. Wang and X. -N. Wang 2012 *Phys. Rev. Lett.* **109** 232301
[8] T. Kalaydzhyan 2014 *Phys. Rev. D* **89** 105012
[9] D.T. Son and P. Surowka 2009 *Phys. Rev. Lett.* **103** 191601
[10] W. Cassing and E. L. Bratkovskaya 2009 *Nucl. Phys. A* **831** 215
[11] E. E. Kolomeitsev, V. D. Toneev and V. Voronyuk 2018 *Phys. Rev. C* **97** 064902
[12] M. I. Baznat, K. K. Gudima, A. S. Sorin and O. V. Teryaev 2016 *Phys. Rev. C* **93** 031902
[13] X. L. Xia, H. Li, Z. B. Tang and Q. Wang 2018 *Phys. Rev. C* **98** 024905
[14] M. Baznat, K. Gudima, A. Sorin and O. Teryaev 2013 *Phys. Rev. C* **88** 061901
[15] O. Teryaev and R. Usubov 2015 *Phys. Rev. C* **92** 014906
[16] A. Sorin and O. Teryaev 2017 *Phys. Rev. C* **95** 011902
[17] M. Baznat, K. Gudima, A. Sorin and O. Teryaev 2018 *Phys. Rev. C* **97** 041902